Downloaded from rsta.royalsocietypublishing.org

PHILOSOPHICAL TRANSACTIONS OF THE ROYAL SOCIETY A MATHEMATICAL, PHYSICAL & ENGINEERING SCIENCES

# Tunnelling Devices as Microwave Mixers and Detectors

R. T. Syme

*Phil. Trans. R. Soc. Lond. A* 1996 **354**, 2351-2364
doi: 10.1098/rsta.1996.0104

**Email alerting service** Receive free email alerts when new articles cite this article - sign up in the box at the top right-hand corner of the article or click **here**

To subscribe to *Phil. Trans. R. Soc. Lond. A* go to:
**http://rsta.royalsocietypublishing.org/subscriptions**

This journal is © 1996 The Royal Society

Downloaded from rsta.royalsocietypublishing.org

# Tunnelling devices as microwave mixers and detectors

By R. T. Syme

*Hirst Division, GEC–Marconi Materials Technology Limited, Elstree Way, Borehamwood, Hertfordshire WD6 1RX, UK*

Semiconductor tunnel devices can be used as mixers or detectors of microwaves and two examples are given in this paper. First, single-barrier tunnel detector diodes are described and their performance is compared with conventional devices at frequencies up to 35 GHz. Second, the predicted and measured performance of resonant tunnelling diodes as mixers at 94 GHz are discussed. Such mixer diodes can exhibit conversion gain but it is shown that their noise figures are, in general, worse than conventional devices. Some conclusions are drawn regarding the likely applications of both kinds of device.

## 1. Introduction

### (*a*) *Detectors and mixers*

A microwave detector is essentially a rectifier of microwaves. For constant amplitude signals it produces a voltage proportional to the microwave power. For an amplitude-modulated signal, it produces a voltage which varies in the same way as the original modulation and so it can be used to extract the information from the microwave signal. Any diode which has a nonlinear current–voltage characteristic can form the basis of a detector, provided it can respond fast enough (to avoid confusion, the term detector is taken to include the detector diode and its associated circuits). At radio frequencies, a p–n junction diode can be used but at the higher microwave frequencies the 'workhorse' device is the metal–semiconductor Schottky diode. Both can be represented by an equivalent circuit consisting of a parallel combination of a resistor $R_j$ and capacitor $C$, in series with another resistor $R_s$ and then an inductor $L$. The resistor $R_j$ and the capacitance $C$ represent the voltage-dependent small-signal resistance and capacitance of the device. The series resistance $R_s$ represents ohmic semiconductor and contact resistances, while $L$ represents a bond-wire inductance. This circuit has a cut-off frequency $f_c$ determined by the time taken to charge/discharge the device capacitance $C$ through the series resistance $R_s$:

$$f_c = (2\pi R_s C)^{-1}. \tag{1.1}$$

The operating frequency $f_0$ should be several times less than $f_c$ for efficient detection.

If the maximum frequency of modulation is $f_m$, then the only frequency range of interest is $f_0 \pm f_m$. However, a detector rectifies noise at all frequencies up to $f_c$ and its 'tangential sensitivity' $T_{ss}$ (which is essentially the minimum detectable signal) is not usually any more than $-55$ dBm at $f_0 = 10$ GHz for a low-noise 1 MHz-bandwidth amplifier after the detector. The noise could be reduced if a filter of bandwidth $2f_m$

*Phil. Trans. R. Soc. Lond.* A (1996) **354**, 2351–2364
*Printed in Great Britain*

© 1996 The Royal Society
TEX Paper

The Royal Society is collaborating with JSTOR to digitize, preserve, and extend access to *Philosophical Transactions: Mathematical, Physical and Engineering Sciences.* www.jstor.org

Downloaded from rsta.royalsocietypublishing.org



centred at $f_0$ was used, but this is difficult when $f_m \ll f_0$. For historical reasons $f_m$ is often referred to as the video frequency, and the impedance of the diode at $f_m$ is called the video impedance. Usually $f_m \ll f_0$ and $f_0 \ll f_c$, so that the video impedance is very close to the small-signal (differential) resistance of the diode at its operating point, i.e. $R_j + R_s \ll 1/(2\pi f_m C)$ in the equivalent circuit.

To increase the signal-to-noise ratio, the signal is first down-converted to an intermediate frequency $f_{IF}$ at which suitable filters and amplifiers are easy to make. The information can then be extracted using a detector with a lower cut-off frequency and hence better $T_{ss}$. The down-conversion process is achieved by mixing the microwave signal with a larger signal from a local oscillator (LO) of slightly different frequency $f_{LO}$; the difference frequency $|f_0 - f_{LO}| = f_{IF}$. As for a detector, a nonlinear device such as a Schottky diode usually forms the basis of the mixer. The down-conversion process will then always involve some loss and additional noise added by the mixer. These are characterized by the mixer's conversion loss $L_c$ and (single-sideband) noise figure $F_{SSB}$; values of $F_{SSB}$ or $L_c$ lower than 6 dB are hard to achieve for $f_0 > 75$ GHz.

The main parameters which characterize detectors and mixers are listed in tables 1 and 2, respectively, along with typical values for conventional diodes and the novel diodes described in §§ 2–3 of this paper.

### (*b*) *Tunnelling diodes*

In most diodes including Schottky diodes and p–n junction diodes, electrons need to get past a potential barrier to get through the device (Sze 1981). The presence of such a barrier to electrons results in a nonlinear current–voltage ($I$–$V$) characteristic. If the barrier height is $V_0$, then classically, only electrons with energy greater than $V_0$ can get over the barrier by thermionic emission or diffusion. For very thin barriers, however, electrons can tunnel through the barrier.

One consequence of this is that the resulting $I$–$V$ characteristic is much less sensitive to changes in temperature. For thermionic emission or diffusion, the electrons with energies greater than $V_0$ are typically deep into the tail of the Fermi–Dirac distribution and so their number varies as $\exp(-V_0/k_B T)$, where $k_B$ is Boltzmann's constant and $T$ is the temperature. The current can therefore be expected to depend exponentially upon the barrier height and the temperature. For tunnelling, however, most of the current is normally carried by electrons below the Fermi energy and the number of such electrons is relatively insensitive to temperature. The probability of tunnelling through the barrier varies approximately as $\exp(-\kappa d)$, where $\kappa = (2m^*[V_0 - E])^{1/2}/\hbar$, $\hbar$ is Planck's constant divided by $2\pi$, $m^*$ is the electron's effective mass, $E$ is its energy and $d$ the barrier thickness. Thus the current can be expected to depend exponentially on the barrier thickness and height, but less strongly upon temperature.

The original 'tunnel diode' was the Esaki diode (Esaki 1958), a p–n junction doped heavily enough such that the majority carriers on each side are degenerate. The tunnel barrier in this case is formed by the bandgap of the semiconductor as the conduction and valence bands bend sharply across the junction. The $I$–$V$ characteristic has a peak and a valley in forward bias. Esaki diodes were investigated extensively for use as microwave sources and amplifiers, owing to their negative differential resistance. However the application for which they are still used today is as a temperature-insensitive, low-impedance, zero-bias detector diode. They usually appear in the form of a backward diode, in which the doping is not quite (or only



PHILOSOPHICAL TRANSACTIONS OF THE ROYAL SOCIETY A MATHEMATICAL, PHYSICAL & ENGINEERING SCIENCES
PHILOSOPHICAL TRANSACTIONS OF THE ROYAL SOCIETY A MATHEMATICAL, PHYSICAL & ENGINEERING SCIENCES

Downloaded from rsta.royalsocietypublishing.org



just) degenerate, so that the current peak in forward bias is essentially absent. The germanium backward detector diode is discussed further in § 2.

For the past 20 years, semiconductor growth techniques have been advancing to the point where atomic layer epitaxy has become a reality. This has opened up a whole new range of heterostructure tunnel devices. The most studied case is the GaAs-based double-barrier resonant tunnelling structure (DBRTS) in which the barriers are made from $Al_xGa_{1-x}As$, with $x$ typically about 0.3 or 1 (pure AlAs). This device has a peak and valley in its $I$–$V$ characteristic, similar to the Esaki diode. However, the physical origin of the peak and valley is different from the Esaki diode and a much wider range of $I$–$V$ characteristics are possible, simply by changing layer thicknesses and materials. This means that much higher frequency operation is possible, with oscillations being observed from a GaAs–AlAs structure above 400 GHz (Brown *et al.* 1989).

Such DBRTS have attracted a lot of interest as possible millimetre-wave sources. Relatively little work has been done on heterostructure tunnel structures as detectors or mixers. In this paper we describe some of our work on both detectors and mixers using tunnelling devices. In § 2, we review the design and testing of single-barrier tunnel structures as microwave detectors up to 35 GHz, while in § 3 we describe some recent work on DBRTS as mixers at 94 GHz. Some brief conclusions are drawn in § 4.

## 2. Microwave detectors using tunnelling diodes

### (*a*) *Design and simulation*

(i) *Basic device structure*

As mentioned in § 1 *b*, the germanium backward diode is still used because of its temperature insensitivity and ability to operate at zero DC bias and present a low video impedance (GaAs Schottky detector diodes have to be DC biased and tend to have video impedances greater than 1 kΩ). The disadvantages are that it has a limited dynamic range, cannot be used much above 30 GHz and is susceptible to burn-out (damage from high power levels). In addition, germanium is a material seldom used for other microwave devices. GaAs-based resonant tunnelling diodes have been investigated as detectors (Gering *et al.* 1988; Mehdi *et al.* 1991), but their performance has not been encouraging. However, a GaAs-based device that combined the advantages of the Ge backward diode with the higher frequency operation and wider dynamic range of a GaAs Schottky diode is desirable.

A device which goes a long way towards meeting this goal is the asymmetric spacer-layer tunnel (ASPAT) diode (Syme *et al.* 1991). This device has a single, very thin AlAs barrier with low-doped GaAs spacer layers of unequal widths on each side. Heavily doped contact regions are present at each end of the device. Since the spacer layers are of unequal length, the voltage is dropped differently across the device for positive and negative bias, as shown in figure 1. Under reverse bias, the end of the device with the longer spacer layer is made positive and most of the voltage drop is after the barrier, across the depleted long spacer. For the opposite polarity, a substantial voltage drop occurs before the barrier so that the effective barrier height is lowered. This qualitative argument explains why one might expect to see an asymmetric $I$–$V$ characteristic. Such asymmetry forms the basis of a detector diode. The capacitance must be such that the operating frequency is much less than $f_c$. For the ASPAT devices discussed here this means that the diodes typically have diameters of less than 15 μm.



PHILOSOPHICAL TRANSACTIONS OF THE ROYAL SOCIETY A MATHEMATICAL, PHYSICAL & ENGINEERING SCIENCES
PHILOSOPHICAL TRANSACTIONS OF THE ROYAL SOCIETY A MATHEMATICAL, PHYSICAL & ENGINEERING SCIENCES

Downloaded from rsta.royalsocietypublishing.org



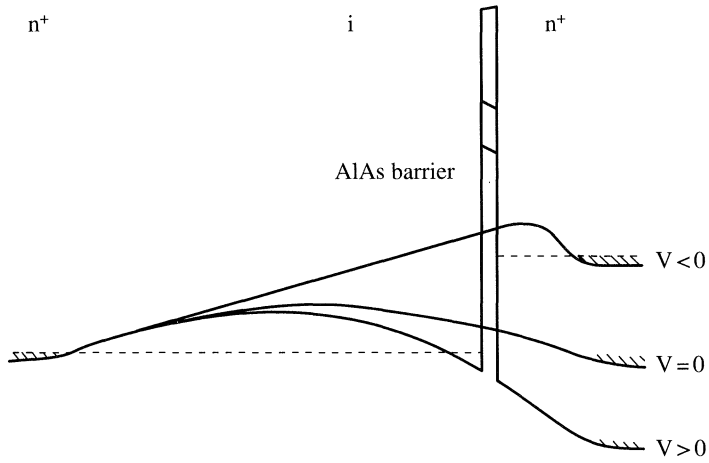


Figure 1. Sketch of conduction band profiles for ASPAT diode at positive, zero and negative bias. The dotted lines represent the chemical potential. For positive bias, the chemical potential is well above the conduction band just before the barrier, so there is an accumulation layer of electrons which can tunnel through. In negative bias no such accumulation layer is present.

(ii) *Calculation of conduction band profile*

A more quantitative prediction of the $I$–$V$ characteristic requires the quantum-mechanically self-consistent solution of Poisson's equation and Schrödinger's equation in the semiconductor in order to calculate the conduction band profile. The method for doing this within an envelope-function approximation (EFA) is described elsewhere (Syme 1993). The EFA treats each semiconductor as a continuous medium. The fact that it is actually a crystal lattice is assumed to be satisfactorily taken into account by assigning an effective mass to the electrons. The part of the wavefunction which oscillates at the lattice periodicity (i.e. the Bloch function) is neglected—only the envelope is considered (somewhat analogous to the amplitude modulation of an RF carrier frequency). This actually turns out to be a very good approximation, even when atomically abrupt interfaces are present, provided that proper account is taken of boundary conditions. The standard boundary conditions on the envelope function $\psi$ are that

$$\psi \text{ is continuous} \tag{2.1}$$

and

$$\frac{1}{m^*(z)}\frac{\mathrm{d}\psi}{\mathrm{d}z} \text{ is continuous,} \tag{2.2}$$

where the $z$ direction is perpendicular to the layers. These are chosen to ensure continuity of current within the EFA.

Calculations have shown (Ando *et al.* 1989) that for an interface between two direct gap semiconductors, such as GaAs–$Al_{0.2}Ga_{0.8}As$, equations (2.1) and (2.2) are a good description of what happens at the interface. A more complicated case is an interface between a direct-gap semiconductor and an indirect-gap semiconductor, such as GaAs–AlAs. In this case, mixing occurs between envelope functions for the three different kinds of conduction band minima and six boundary conditions must be satisfied (Ando & Akera 1989).

Once the boundary conditions are properly treated, deviations from the EFA are negligible compared with effects such as uncertainty in band offsets and non-

Downloaded from rsta.royalsocietypublishing.org



parabolicity. Refinements within the EFA are possible to account for these additional effects.

In the work described in this paper, equations (2.1) and (2.2) have been used for GaAs–AlAs interfaces since most electrons stay in the Γ-valley as they travel through the very thin AlAs layers. Some electrons do transfer to the X-valley in the AlAs but this does not have any significant effect upon the conduction band profile (although it does affect the current—see the next section).

For each value of bias a different conduction band profile is obtained. For forward bias (the side with long spacer is negative), the conduction band bends so much before the barrier that an accumulation layer is formed, made up from electrons in quasi-two-dimensional states.

(iii) *Calculations of I–V characteristics*

Once the conduction band profile has been calculated, the current is calculated from the following expression, assuming that an accumulation layer is formed before the barrier containing $N$ quasi-two-dimensional states:

$$J = \sum_{i=1}^{N} \frac{2m^* e E_i (1 - R_i) k_B T}{\pi^2 \hbar^3} \ln \left[ \frac{1 + \exp((E_F - E_i)/k_B T)}{1 + \exp((E_F - E_i - eV)/k_B T)} \right]. \tag{2.3}$$

The additional current arising from electrons in continuum states can be calculated using a similar expression, with the sum replaced by an integral over the continuum states.

As mentioned above, most of the electrons remain in the Γ-valley, with the probability of transfer to the X-valley in the AlAs being of the order of $10^{-4}$ (Othaman *et al.* 1993). However, the current due to electrons which transfer to the X-valley in the AlAs turns out to be an important contribution, since the Γ–Γ conduction band offset is approximately 1.0 eV, while the Γ–X offset is only 0.16 eV.

## (*b*) *Device fabrication and testing*

(i) *Device fabrication*

All the material was grown on $n^+$ GaAs substrates by either molecular-beam epitaxy (MBE) or metal-organic chemical-vapour deposition (MOCVD). Large-area devices (100 μm diameter) were fabricated for DC assessment using mesa etching and annealed AuGeNi contacts. For microwave testing, diodes ranging in size from 8 to 20 μm diameter were fabricated using mesa etching and $SiO_2$–$Si_3N_4$ passivation. Again, AuGeNi was used to make ohmic contacts. For frequencies up to 20 GHz, chips were bonded into ceramic packages and covered in a protective epoxy coating. For testing at 35 GHz, beam-lead devices were produced.

(ii) *DC assessment*

The measured current–voltage characteristics of three ASPAT structures are shown in figure 2. Sample DB1220 is MBE-grown, while E20291 and E20396 were grown by MOCVD. For E20396, video impedances similar to those of germanium backward diodes (300 Ω) are easily achievable at zero bias and $f_c$ is a factor of two higher, owing to the smaller capacitance of the ASPAT structure. The other structures in figure 2 had thicker AlAs barriers (about 4 nm for DB1220) but similar doping profiles to E20396. Thus their video impedance is considerably larger, of the order of 10 kΩ.

Downloaded from rsta.royalsocietypublishing.org



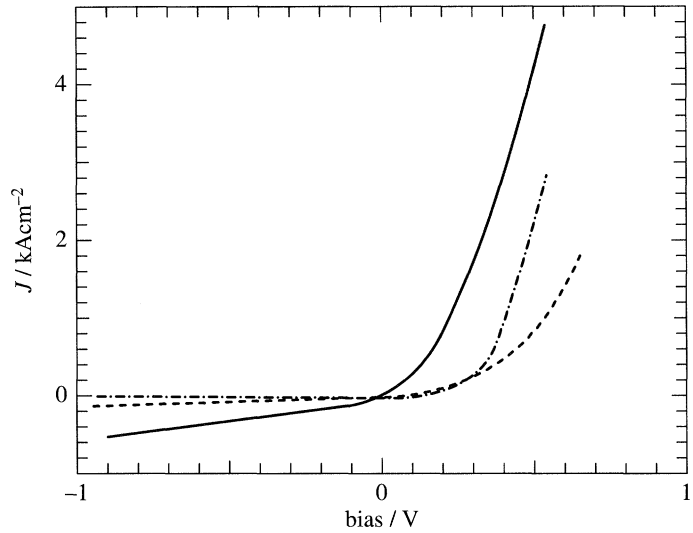


Figure 2. Measured current density–voltage characteristics of three ASPAT structures. Note the asymmetry.

(iii) *Microwave assessment*

Diodes were placed in a simple microstrip circuit on either alumina or quartz substrates. A short circuit at the RF was provided at the diode by an open circuit, quarter-wavelength stub. The results of testing at 9.4 GHz have been presented before (Syme *et al.* 1992), and are summarized in table 1. Figure 3 shows examples of the transfer function at 9.4 GHz for ASPAT E20396 and some conventional diodes. The response is similar to a zero-bias silicon Schottky diode with a better voltage sensitivity than the germanium backward diode. The variation of the voltage sensitivity with temperature (from −40 °C to +80 °C)is considerably better at 1.3 dB than the Schottky diode (3.3 dB) but not as good as the backward diode (0.3 dB). The variation with temperature for the ASPAT diode is almost entirely due to the current associated with electrons transferring to the X-valley: once in the X-valley, electrons see only the 0.16 eV barrier and so transport tends to occur by thermionic emission rather than tunnelling at room temperature. The dynamic range of the ASPAT diode is more than 20 dB better than the backward diode, as can be seen from figure 3 and the fact that they both have tangential sensitivities of about −53 dBm.

At 35 GHz, the results are qualitatively similar. The voltage sensitivity decreases by about 3 dB for the ASPAT diodes but by about 6 dB for the zero-bias Si Schottky diodes. The backward diodes do not work at 35 GHz. Thus at 35 GHz, the ASPAT diodes has as good a sensitivity as the best of the other types of diode, but has a variation with temperature that is only half as much as its nearest competitor, the planar-doped barrier diode.

## 3. Microwave mixers at 94 GHz using double-barrier diodes

### (*a*) *Design and simulation*

(i) *Basic device structure and mode of operation*

In § 1, the use of double-barrier structures as mixer diodes was mentioned. The idea behind this is to use the negative differential resistance (NDR) region of the

Downloaded from rsta.royalsocietypublishing.org



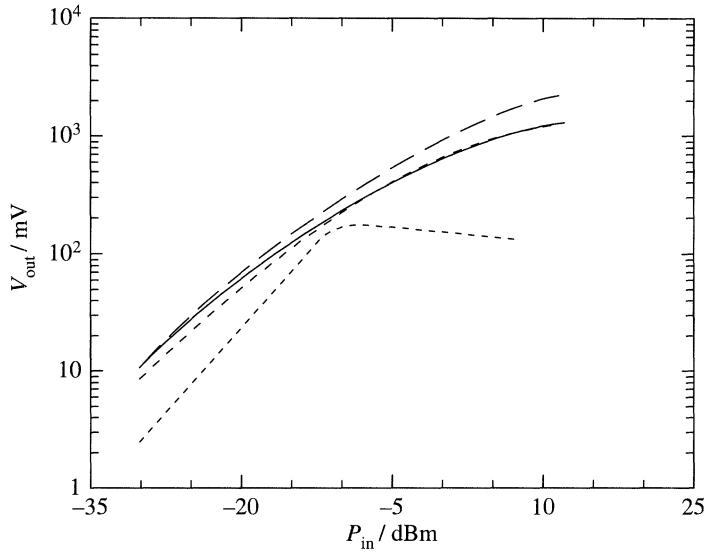


Figure 3. Comparison of the performance of microwave detectors at 9.4 GHz including ASPAT structure E20396.

Table 1. *Comparison of conventional detector diodes and* ASPAT *diodes at 9.4 GHz*

($T_{ss}$ is the tangential sensitivity, $\beta_v$ is the voltage sensitivity, $P_{1dB}$ is the power at which the output voltage has dropped 1 dB below its extrapolated value and $\Delta V(T)$ is the variation in output voltage between −40 °C and +80 °C. All diodes are operated at zero bias, including the planar-doped barrier (PDB) diode. )

| device | $T_{ss}$ (dBm) | $\beta_v$ ($VW^{-1}$) | $P_{1dB}$ (dBm) | $\Delta V(T)$ (dB) |
|---|---|---|---|---|
| Ge back diode | −52 | 3000 | −11 | 0.3 |
| Si Schottky | −54 | 6000 | 8 | 3.3 |
| PDB | −56 | 6000 | 10 | 2.2 |
| DB1220 | −44 | 800 | 12 | 1.1 |
| E20291 | −53 | 5200 | 10 | 1.2 |
| E20396 | −53 | 2400 | 12 | 1.5 |

diode as an 'amplifier' in order to improve the conversion loss of the mixer. Such operation has been investigated for Esaki diodes many years ago and more recently for DBRTS at frequencies up to 18 GHz (Hayes *et al.* 1993). The diode is biased at some point usually just outside the NDR region and the local oscillator applied so that the LO voltage sweeps across some or all of the NDR region. The resulting small-signal impedances at the signal and IF have a negative real part, making amplification possible. Operation as self-oscillating mixers has also been investigated (Robertson & Lesurf 1991; Millington *et al.* 1991).

The basic structure of the DBRTS used in this work is similar to the ASPAT diode, except that there are two AlAs barrier separated by a GaAs or InGaAs quantum well and the spacer layers are not always so asymmetric. The AlAs barrier thickness and the doping profile are designed so as to adjust the peak current density to a desired value. The length of the spacer regions is primarily determined by the capacitance

Downloaded from rsta.royalsocietypublishing.org



required. The thickness of the quantum well is chosen so that the bound levels are far enough apart that only one peak is seen in the $I$–$V$ characteristic. Further details of the design are given in the next section.

The same equivalent circuit as a detector diode is applicable but with $R_j$ replaced by $-R_j$, the negative resistance. There is therefore a cut-off frequency given by (1.1), as for a detector diode. There are, however, two other characteristic frequencies of importance for a negative resistance mixer. The first is the frequency at which the real part of the impedance becomes positive and it is given by

$$f_{\mathrm{R}} = \frac{1}{2\pi r_j C}\sqrt{\frac{R_j}{R_{\mathrm{s}}} - 1}. \tag{3.1}$$

For any advantage to be obtained from using the negative resistance, the operating frequency must clearly be less than $f_{\mathrm{R}}$. The second is the self-oscillation frequency at which the imaginary part of the impedance becomes zero:

$$f_{\mathrm{X}} = \frac{1}{2\pi R_j C}\sqrt{\frac{R_j^2 C}{L} - 1}. \tag{3.2}$$

For small-signal stability $f_{\mathrm{X}}$ must be greater than $f_{\mathrm{R}}$. This turns out to be difficult to satisfy for 94 GHz devices using conventional processing techniques. To increase these characteristic frequencies it is important to have a small capacitance $C$, while a high $f_{\mathrm{X}}$ requires a low series inductance $L$. For a beam-lead diode, $L$ is approximately 0.1 nH. The smallest area beam-lead diodes which we could readily make were 6 μm in diameter. For a total distance between the contacts of 200 nm, this gives $C = 16$ fF. The value of the series resistance $R_{\mathrm{s}}$ is unlikely to be less than 5 Ω for the type of structure considered, while $R_j$ should be in the region of 50–300 Ω in order to match the diode reasonably well to the circuit. Taking $R_j$ to be 200 Ω gives $f_{\mathrm{R}} = 310$ GHz and $f_{\mathrm{X}} = 115$ GHz. Thus 94 GHz operation is feasible in that $f_{\mathrm{R}}$ is considerably greater than 94 GHz, but small-signal stability would appear difficult to achieve. Small-signal stability can be achieved by increasing $R_{\mathrm{s}}$, at the expense of reducing the maximum operating frequency (e.g. with $R_{\mathrm{s}} = 32$ Ω and other component values unchanged, $f_{\mathrm{R}} = 114$ GHz while $f_{\mathrm{X}}$ is unchanged).

Although this situation is undesirable, it is not necessarily a problem because a mixer is driven by a large signal—the local oscillator. The LO drive alters the effective small-signal impedance seen by the RF (primarily by altering $R_j$) so that one has an extra degree of freedom in trying to find a stable operating point. When the first terms inside the square root in (3.1) and (3.2) are much greater than unity, $f_{\mathrm{R}} \propto 1/\sqrt{R_j}$, while $f_{\mathrm{X}}$ becomes independent of $R_j$. Thus if $R_j$ is increased (reduced), $f_{\mathrm{R}}$ tends towards becoming smaller (larger) than $f_{\mathrm{X}}$ and so the diode can be expected to become more stable (unstable).

(ii) *Simulation of $I$–$V$ characteristics and mixer performance*

The $I$–$V$ characteristics of the DBRTS were simulated in a similar way to those of the detector diodes described in § 1, except that full quantum-mechanical self-consistency in the quantum well was not considered. The neglect of scattering in double-barrier structures leads to an underestimate of the valley current. When the device is biased in the valley region, the bound level in the quantum well is not accessible to electrons from the emitter contact unless they lose energy. If they can scatter down close to the bound level, they have an easy route through the structure.



PHILOSOPHICAL TRANSACTIONS OF THE ROYAL SOCIETY A MATHEMATICAL, PHYSICAL & ENGINEERING SCIENCES
PHILOSOPHICAL TRANSACTIONS OF THE ROYAL SOCIETY A MATHEMATICAL, PHYSICAL & ENGINEERING SCIENCES

Downloaded from rsta.royalsocietypublishing.org



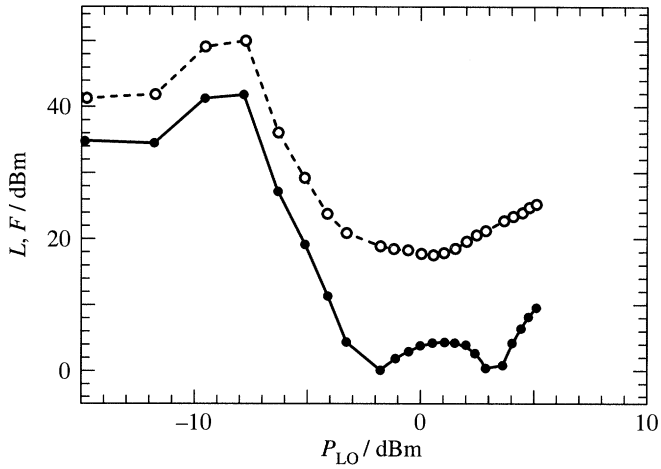


Figure 4. Predicted mixer performance of a GB1247 diode at a bias of 1.8 V.

Hence a significantly larger valley current can be expected than is predicted within a model without scattering. The peak current is not affected in this way by inelastic scattering.

The simulated $I$–$V$ characteristics were used to model the mixer action of the devices. A modified version of the model of Siegel & Kerr (1979) was used. The predicted mixer performance of structure GB1247 is shown in figure 4 for a bias just below the peak. The important features are that a conversion loss $L_c$ close to 0 dB is predicted, but that the single-sideband noise figure $F_{SSB}$ is poor, the best predicted value being 18 dB. No significant improvement in noise figure was found by changing the bias.

(iii) *The problem of high noise figure*

It became clear that shot noise was dominating the SSB noise figure. Although proper calculation of the noise figure (or, equivalently, the noise temperature) requires a model such as that of Siegel & Kerr (1979), the diode noise–temperature ratio (NTR) may be estimated more easily. For a Schottky diode, it is well known that the NTR is predicted to be $0.5n$ ($n$ being the ideality factor), but values closer to unity tend to be measured. One way of obtaining the NTR is as follows. The shot noise power generated by the diode in bandwidth $\Delta f$ is

$$P_{\text{shot}} = \frac{eI\Delta f}{2(\mathrm{d}I/\mathrm{d}V)}, \tag{3.3}$$

and so the equivalent noise temperature is given by

$$T_{\text{shot}} = \frac{P_{\text{shot}}}{k_{\text{B}}\Delta f} = \frac{eI}{2k_{\text{B}}(\mathrm{d}I/\mathrm{d}V)}. \tag{3.4}$$

The important quantity is therefore

$$\frac{\mathrm{d}I/\mathrm{d}V}{I} = \frac{\mathrm{d}\ln I}{\mathrm{d}V} = \frac{1}{IR_j}, \tag{3.5}$$

which should be as large as possible for low noise. For a Schottky diode,

$$\frac{\mathrm{d}\ln I}{\mathrm{d}V} \approx \frac{e}{nk_{\text{B}}T} \tag{3.6}$$

Downloaded from rsta.royalsocietypublishing.org



provided that $I$ is much greater than the saturation current, and so the NTR is equal to $0.5n$ (as stated above). For DBRTS, however, $\mathrm{d}\ln I/\mathrm{d}V$ is typically about 10 times smaller, e.g. for $\mathrm{d}V/\mathrm{d}I = 200\,\Omega$ and $I = 1$ mA, $\mathrm{d}\ln I/\mathrm{d}V = 5$. Hence for $n = 1.1$, the NTR of the DBRTS would be 8 dB higher.

This is a consequence of the fact that the nonlinearity in the NDR of the double-barrier diode's $I$–$V$ characteristic is weak compared with that of a Schottky diode. In order to get the benefit from the NDR, the LO should sweep over a substantial part of the NDR, but in order to get a large nonlinearity, the LO should only sweep over the region near the peak or near the valley. However, the real part of the diode impedance changes from very large positive to very large negative at the peak and valley, so that the impedance averaged over one LO cycle seen by the RF signal would tend to be very large. This makes matching the diode difficult.

One could try reducing the operating current without increasing $\mathrm{d}V/\mathrm{d}I$. For example, one could let the operating current be 0.2 mA and keep $\mathrm{d}V/\mathrm{d}I$ down at 200 Ω. If we say that this is about half the peak current and that the peak-to-valley ratio is 3 then we obtain an estimate of the peak–valley voltage difference as 53 mV (assuming $\mathrm{d}V/\mathrm{d}I$ in the whole NDR region is 200 Ω). The predicted (and measured) peak–valley voltage separation of the first structure designed (GB1247) is approximately 600 mV, and so we see that the voltage scale needs to be contracted. The problem with doing this is the presence of the spacer regions. These are required in order to reduce the capacitance but they have the effect of expanding the voltage scale of the $I$–$V$ characteristic. However, by making the spacer layers asymmetric (as for the ASPAT diode), the voltage scale for one bias direction is contracted. This was done in structure GB1309, resulting in a predicted peak–valley voltage separation of *ca.* 0.1 V. The best noise figure predicted from the modelled $I$–$V$ characteristic of GB1309 was 15 dB. Although some additional benefit could be obtained by reducing $\mathrm{d}V/\mathrm{d}I$ in the NDR region, this has the unwanted side-effect of making the diode more unstable.

In order to reduce the peak-to-valley voltage separation further, a structure (GB1442) was modelled with an InGaAs well between the two AlAs barriers. Since the bandgap of InGaAs is smaller than GaAs, the bound level in the well occurs at a lower energy relative to the conduction band in the emitter contact. This means that the NDR region should occur at a lower voltage than for the same structure with a GaAs well and that the drop in current between peak and valley should be sharper. Peak to valley voltage separations of less than 100 mV were predicted, and a best modelled noise figure of 8 dB.

As described in the previous section, the approach towards instability with change in LO power can be associated with a reduction in $\mathrm{d}V/\mathrm{d}I$ ($= R_j$). One prediction from the above is therefore that the lowest noise figure may occur at a bias and LO power close to where the diode becomes unstable. This somewhat counterintuitive prediction is in agreement with the experimental results described below.

### (*b*) *Device fabrication and testing*

#### (i) *Device fabrication and DC assessment*

All structures were grown by MBE on $n^+$ GaAs substrates. Beam-lead diodes were fabricated with mesa diameters in the range 5–9 μm. Representative $I$–$V$ characteristics for the three double-barrier structures discussed above are shown in figure 5. It should be noted how the peak-to-valley voltage separations and peak voltages are smaller for the latter structures. Modelling of the mixer performance was carried

Downloaded from rsta.royalsocietypublishing.org



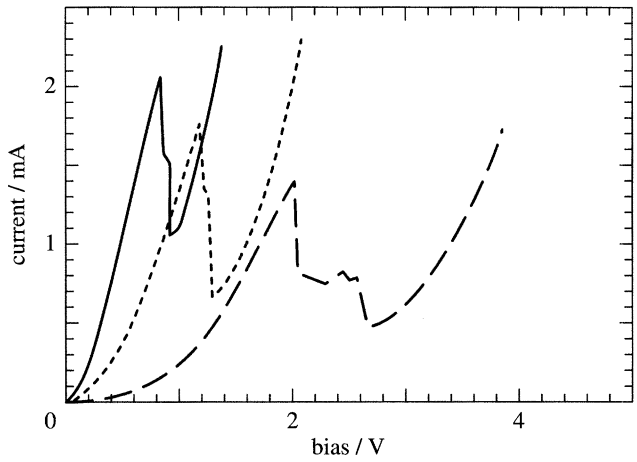


Figure 5. Current–voltage characteristics of resonant tunnelling mixer diodes made from GB1247, GB1309 and GB1442. Note how the voltage scale has reduced for each diode in turn.

out using these experimental $I$–$V$ characteristics. These modelled values for $L_c$ and $F_{SSB}$ were in line with the predictions based upon the modelled $I$–$V$ characteristics, except that the best noise figure for GB1442 (the InGaAs-containing structure) was 12 dB (rather than 8 dB).

(ii) *Microwave assessment*

The beam-lead diodes were bonded into small suspended-microstrip circuits on 0.005 inch thick quartz substrates, measuring 10 mm by 1.5 mm. These substrates were then mounted in a block in which WG27 waveguide was machined. The substrates were placed across the waveguide so that RF and LO could couple into the suspended microstrip and hence into the diode. Filter sections at each end of the circuit prevented RF or LO leakage.

The LO was coupled into this single-ended mixer by combining it with the RF signal in a 10 dB coupler, giving a 10 dB isolation of LO AM noise. Isolators were used in the waveguide circuit to prevent reflected LO power entering the RF source. For noise figure measurements, a W-band noise tube was used with an excess noise ratio of 14.2 dB. A standard double Y-factor method was used for obtaining the conversion loss and noise figure simultaneously (Maas 1993). The conversion loss was also obtained using direct measurement of the IF power for an RF input power of typically −25 dBm. The frequency-dependent losses in the IF and RF circuits were measured and corrections made to account for such losses. This is in an attempt to be able to remove the circuit effects and compare different diodes. It is estimated that the values quoted below have an experimental uncertainty of less than 0.3 dB.

In order to check the measurement system, a well-characterized Schottky diode mixer was assessed. The values obtained for $L_c$ and $F_{SSB}$ were 7.5 and 8.7 dB, in agreement with previous measurements. This offers a benchmark against which to judge the performance of the DBRTS mixers.

The conversion loss as a function of LO power for a GB1247 diode and a GB1442 diode are shown in figure 6 for biases just above the valley in both cases and an input power of −25 dBm. Conversion gain is achieved for GB1442, but with a very sharp peak as a function of LO power. The conversion loss of GB1247 is also good at 3 dB and peaks somewhat less sharply. This would appear to be the first observation

Downloaded from rsta.royalsocietypublishing.org



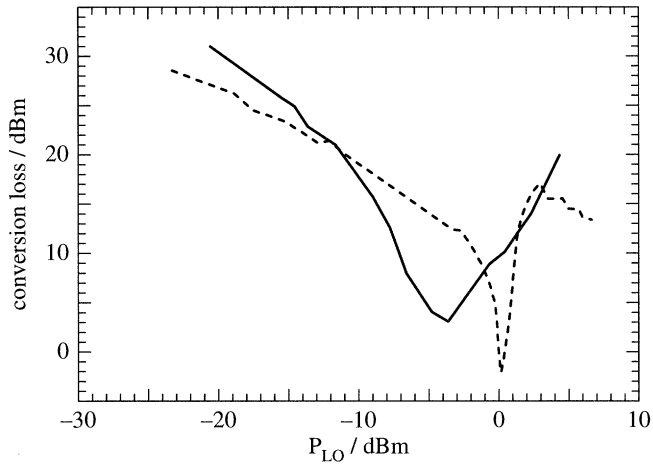


Figure 6. Conversion loss versus LO power for a GB1247 diode and a GB1442 diode at 94 GHz.

Table 2. *Comparison of conventional mixer diodes and DBRTS diodes at 94 GHz*

($L_c$ is the conversion loss (negative for gain), $T_{SSB}$ is the single-sideband noise temperature and $F_{SSB}$ is the single-sideband noise figure (defined here as $1 + T_{SSB}/T$]. $P_{L3dB}$ is defined as the range of LO power for which $L_c$ is within 3 dB of its best value—this shows how sharply peaked $L_c$ is for the DBRTS mixers.)

| device | $L_c$ (dB) | $T_{SSB}$ (K) | $F_{SSB}$ (dB) | $P_{L3dB}$ (dB) |
|---|---|---|---|---|
| GaAs Schottky | 8 | 2000 | 9 | 10 |
| GB1247 | 3 | 36 000 | 21 | 3 |
| GB1309 | 1 | 8800 | 15 | 2 |
| GB1442 | −2 | 3400 | 11 | 1 |

of conversion gain from such devices at W-band frequencies. The 1 dB compression point (for the linearity of the conversion process) occurs at an RF power in the region of −20 to −25 dBm. The conversion loss/gain as a function of IF varied by less than 0.5 dB between −1.2 GHz and +1.2 GHz.

As predicted, the noise figures were not so encouraging. The best values mostly occurred when the conversion figure was at its best, and this tended to be a bias and LO power close to where the diode became unstable. The typical values obtained are given in table 2. The best measured value was $F_{SSB} = 8$ dB, for a GB1442 diode. However this value was difficult to reproduce, was extremely sensitive to bias and was found in only one diode (the second best noise figure was 10 dB).

## 4. Conclusions

The ASPAT diode described in § 2 show promise as a microwave detector whose performance varies only slightly with temperature. The variation due to temperature could be reduced by using a material system in which a small band offset was not available to the electrons in any of the conduction band valleys. This is the case for AlInAs–GaInAs lattice matched to InP, and for some of the antimony based semiconductors. Alternatively, a compromise in the GaAs–AlGaAs system might be

Downloaded from rsta.royalsocietypublishing.org



achieved by using an Al content somewhere between 60% and 90%. The main factor determining whether or not such diodes will get produced is their manufacturability. It is not clear whether structures can be reliably and repeatably produced when they contain AlAs layers only 2–4 nm thick which need to have their thickness correct to one monolayer. However, recent work (Wilkinson *et al.* 1996) does suggest that growth techniques have advanced sufficiently to make this possible.

Double-barrier diodes have been shown to have conversion gain as mixers at 94 GHz. However, that conversion gain is sharply peaked as a function of bias and LO power. Even if a conversion loss of 3 dB is allowed, the conversion loss was observed to worsen by 1 dB for a 1 dB change in LO power. More of a problem is the poor noise figure of double barrier mixer diodes at 94 GHz. This is due to shot noise, and, as discussed in this paper, it is difficult to reduce the shot noise while maintaining a high cut-off frequency and stable operation. There is no scope for a compromise between stable operation, conversion loss and noise figure at 94 GHz. Even if very small area diodes could be made with low parasitic reactances, it seems unlikely that a noise figure of better than 8 dB could be achieved. In addition, the performance would be too sensitive to LO power to be of practical use. Therefore, although double barrier diodes do not suffer the same frequency limitations as Esaki diodes, it seems likely that they will follow the same path and not show sufficient advantage over Schottky diodes for them to be used in mixers. Low-noise frequency conversion with gain at millimetre-wave frequencies will not be achieved with negative resistance diodes, but will probably occur with further improvements in GaAs monolithic FET-based circuits.

The work on ASPAT diodes took place as part of a programme entitled 'New Quantum Electronic Devices' and was jointly funded by the Department of Trade and Industry under its GaAs Advanced Technology Initiative and by GEC Plessey Semiconductors. The mixer work has been carried out with the support of the Defence Research Agency, Malvern. Semiconductor wafers were grown by GEC–Marconi Materials Technology and Epi Materials Ltd. All microwave devices were fabricated at GEC Plessey Semiconductors. Some of the work on ASPATs was carried out at the University of Cambridge while the author was on secondment there. I would particularly like to thank the following for their involvement in this work: K. J. Ming, B. Kumar, R. S. Smith (GMMT); M. J. Kelly (University of Surrey); M. Pepper (University of Cambridge); A. W. Higgs, D. G. Hayes (DRA); I. Dale and M. Carr (GPS).

## References

Ando, T., Wakahara, S. & Akera, H. 1989 Connection of envelope functions at semiconductor heterointerfaces. I. Interface matrix calculated in simplest models. *Phys. Rev.* B **40**, 11 609–11 618.

Ando, T. & Akera, H. 1989 Connection of envelope functions at semiconductor heterointerfaces. II. Mixings of Γ and X valleys in GaAs/$Al_xGa_{1-x}As$. *Phys. Rev.* B **40**, 11 619–11 633.

Brown, E. R., Sollner, T. C. L. G., Parker, C. D., Goodhue, W. D. & Chen, C. L. 1989 Oscillations up to 420 GHz in GaAs/AlAs resonant tunnelling diodes. *Appl. Phys. Lett.* **55**, 1777–1779.

Esaki, L. 1958 New phenomenon in narrow germanium p–n junctions. *Phys. Rev.* **109**, 603–604.

Gering, J. M., Rudnick, T. J. & Coleman, P. D. 1988 Microwave detection using the resonant tunnelling diode. *IEEE Trans. Microwave Theory Technol.* **36**, 1145–1150.

Hayes, D. G., Higgs, A. W., Wilding, P. J. & Smith, G. W. 1993 Conversion gain at 18 GHz from resonant tunnelling diode mixer operated in fundamental mode. *Electron. Lett.* **29**, 1370–1372.

Maas, S. A. 1993 *Microwave mixers*, 2nd edn, pp. 95–203. Boston, MA: Artech House.

Mehdi, I., East, J. R. & Haddad, G. I. 1991 Characterisation of resonant tunnelling diodes for microwave and millimeter-wave detection. *IEEE Trans. Microwave Theory Tech.* **39**, 1876–1880.



PHILOSOPHICAL TRANSACTIONS OF THE ROYAL SOCIETY A MATHEMATICAL, PHYSICAL & ENGINEERING SCIENCES

PHILOSOPHICAL TRANSACTIONS OF THE ROYAL SOCIETY A MATHEMATICAL, PHYSICAL & ENGINEERING SCIENCES

Downloaded from rsta.royalsocietypublishing.org



Millington, G., Miles, R. E., Pollard, R. D., Steenson, D. P. & Chamberlain, J. M. 1991 A resonant tunnelling diode self-oscillating mixer with conversion gain. *IEEE Microwave Guided Wave Lett.* **1**, 320–321.

Othaman, Z., Geim, A. K., Bending, S. J., Syme, R. T. & Smith, R. S. 1993 Unambiguous identification of X-point-related resonances in GaAs/AlAs/GaAs tunnel diodes under hydrostatic pressure. *Semicond. Sci. Technol.* **8**, 1483–1486.

Robertson, M. R. & Lesurf, J. C. G. 1991 Self-oscillating mixing in a QW double barrier diode at W-band. *Int. J. Infrared mm-waves* **12**, 1379–1385.

Siegel, P. H. & Kerr, A. R. 1979 A user oriented program for the analysis of microwave mixers and a study of the effects of the series inductance and diode capacitance on the performance of some simple mixers. *NASA Technical Memorandum* **80324**.

Syme, R. T. 1993 Microwave detection using GaAs/AlAs tunnel structures. *GEC J. Res.* **11**, 12–23.

Syme, R. T., Kelly, M. J., Smith, R. S., Dale, I. & Condie, A. 1991 A tunnel diode with asymmetric spacer layers for use as a microwave detector. *Electron. Lett.* **27**, 2192–2194.

Syme, R. T., Kelly, M. J., Robinson, M. F., Smith, R. S. & Dale, I. 1992 Novel GaAs/AlAs tunnel structures as microwave detectors. *Proc. SPIE* **1675**, 46–56.

Sze, S.M. 1981 *Physics of semiconductor devices*, 2nd edn, ch. 2 and 5. New York: Wiley.

Wilkinson, V. A., Kelly, M. J. & Kidd, P. 1996 Growth, characterisation and manufacturability of microwave tunnel diodes. (To be published in *Proc. Int. Conf. on Semiconductor Heteroepitaxy* (July 95, Montpellier).)



PHILOSOPHICAL TRANSACTIONS OF THE ROYAL SOCIETY A MATHEMATICAL, PHYSICAL & ENGINEERING SCIENCES

PHILOSOPHICAL TRANSACTIONS OF THE ROYAL SOCIETY A MATHEMATICAL, PHYSICAL & ENGINEERING SCIENCES